

Indirect searches for dark matter particles with the Super-Kamiokande detector

K. FRANKIEWICZ on behalf of the SUPER-KAMIOKANDE COLLABORATION

National Centre for Nuclear Research, Warsaw, Poland

Summary. — A search for dark matter (DM) induced neutrinos from the Milky Way has been performed based on data collected with the Super-Kamiokande detector in years 1996-2014. Dark matter density is expected to be largely enhanced in the area of the Galactic Center (GC) which may result in increased annihilation/decay of relic particles in that region. The analysis focuses on the search for angular anisotropy in the number of observed neutrino events between the GC and the other part of the sky where the expected flux of dark matter annihilation/decay products is low. No excess of neutrinos from the GC region has been observed with respect to atmospheric neutrino background. Upper limits on the self-annihilation cross-section and lower limits on the lifetime have been obtained for dark matter particle masses ranging from 1 GeV to 10 TeV for various dark matter halo models.

PACS 13.15.+g – Neutrino interactions.

PACS 95.35.+d – Dark matter (stellar, interstellar, galactic, and cosmological).

1. – Dark matter detection

Detection and elucidating the nature of DM is one of the main goals of the astrophysics and particle physics nowadays. There are two main strategies for DM detection - direct and indirect. The direct methods are based on the assumption that DM particles can be elastically scattered on the baryonic nuclei. Many experiments attempt to measure the kinetic energy of resulting nuclear recoils. Current results are inconsistent and controversial. Indirect searches aim at detection of DM annihilation/decay products in the fluxes of cosmic rays, such as charged particles, photons or neutrinos. The latter, can be produced directly or in subsequent decays of mesons and leptons.

Neutrinos can provide very good information on their source position while traversing unaffected through galactic scales. Moreover, their energy remain completely unchanged during propagation providing valuable information about energy spectra generated in DM annihilation/decay processes. On the other hand, detection of neutrinos is very challenging due to their weak-scale cross section and the fact that they are neutral and one relies on observation of products of their interactions.

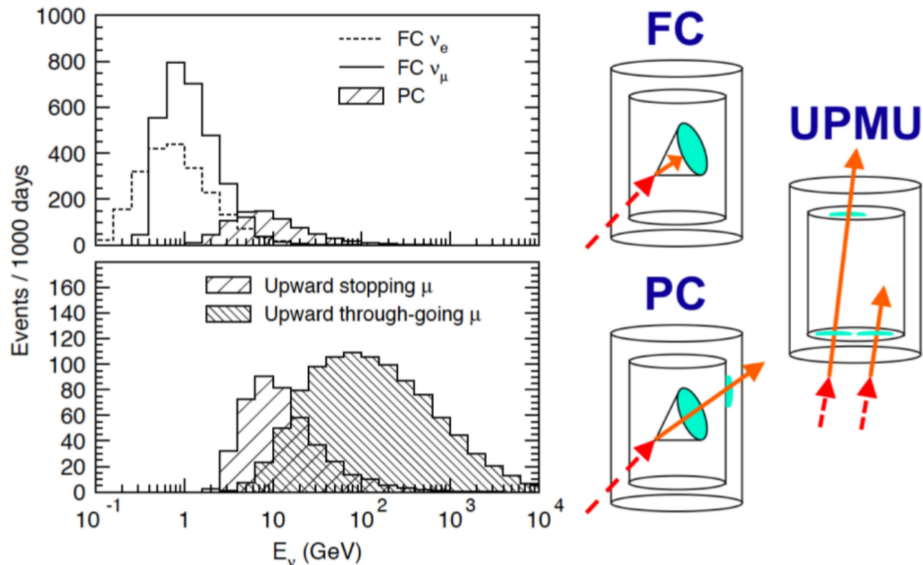


Fig. 1. – The expected true neutrino energy distributions for the fully-contained, partially-contained (upper plot), upward stopping and upward through-going muons samples (lower plot) [1].

2. – Super-Kamiokande detector and atmospheric neutrinos

Super-Kamiokande (SK) is a 50 kton water Cherenkov detector located at the Kamioka Observatory of the Institute for Cosmic Ray Research, University of Tokyo [2]. The observatory was designed to search for a proton decay, study solar, atmospheric and man-made neutrinos, and keep watch for supernovae. Detection of neutrino interactions is based on observation of charged particles, primarily leptons, which may produce Cherenkov radiation while moving faster than c in water. The Cherenkov light projected onto the walls of the detector and recorded by photomultipliers, allows to reconstruct energy, direction and flavour of a parent neutrino.

Among all neutrino sources it is worth to discuss atmospheric neutrinos as they have the same energy range as it is expected for DM induced neutrinos. Atmospheric neutrinos are produced in interactions of cosmic rays with atomic nuclei in the Earth's atmosphere. Their average energy is of several hundreds of MeV and the energy spectra has a long high energy tail reaching TeV scale. If the charged lepton produced in neutrino interaction stops in the inner detector, this type of event is classified as fully-contained (FC). If a high energy lepton exits the inner detector and deposits energy also in the outer veto region, event is classified as partially-contained (PC). The energies of PC events are typically 10 times higher than those producing FC events. Neutrinos also interact with the rock surrounding the detector and may produce high energy muons which intersect the tank. Downward-going muons produced in interactions of neutrinos cannot be distinguished from the constant flux of cosmic ray muons. However, muons travelling in upward direction (UPMU) must be neutrino induced. The expected number of neutrino events in each class is presented in Fig. 1 as a function of neutrino energy. The discussed analysis is based on atmospheric neutrino data collected with SK detector in

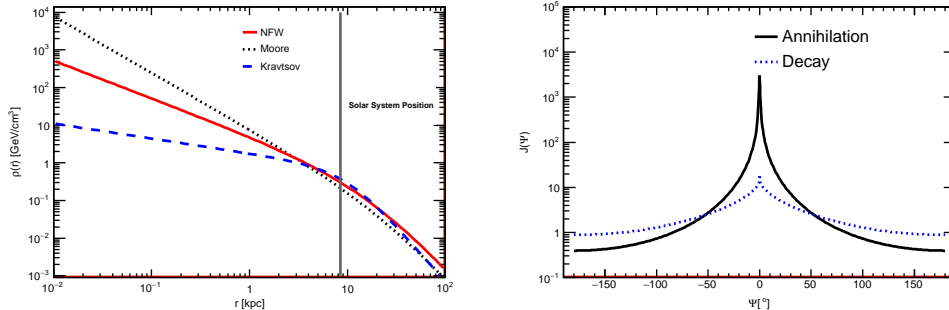


Fig. 2. – Left plot: DM density ρ vs distance from the GC for three halo profiles (NFW [3] (red-solid), Moore [4] (black-dotted) and Kravtsov [5] (blue-dashed)) considered in the analysis. Right plot: Expected intensity $J(\Psi)$ of DM annihilation (black-solid)/decay (blue-dotted) products for NFW halo model as a function of angular distance Ψ .

years 1996-2014 (SK-I, SK-II, SK-III and SK-IV data taking periods), corresponding in total to 4223.3 livetime-days for FC/PC and 4527.0 livetime-days for UPMU events.

3. – Dark matter halo and signal simulation

The intensity of expected DM induced neutrino signal is proportional to the square of the DM density in the halo (in case of annihilation) or to the density (in case of decay) (see Fig. 2, right plot). Therefore, the distribution of DM in the Milky Way is crucial for any robust predictions. It is expected that DM halo envelops the galactic disk and extends far beyond the edge of the visible galaxy. The three commonly used profiles: Navarro-Frenk-White [3], Moore [4] and Kravtsov [5] are obtained as a result of cosmological N-body simulations with large dynamic range [6] and gravitational lensing observations [7]. The comparison of DM density distribution, $\rho(r)$, as a function of the distance from the GC for the considered profiles is shown in Fig. 2 (left plot). For the outer regions of the halo (several kpc away from the GC) one observes good agreement between profiles. However, the inner gradients of the halo profiles are the most uncertain part, due to the spatial resolution limit of existing simulations. In the presented analysis, the NFW is used as a benchmark model, while the Moore and Kravtsov profiles are applied as extreme cases to estimate the influence of halo model choice on the obtained results. Since DM halo profiles are peaked towards the GC one expects very large enhancements for small angles around this point.

The differential flux of annihilation products with average intensity $J_{\Delta\Omega}$, can be expressed in the form [8]:

$$(1) \quad \frac{d\Phi_{\Delta\Omega}}{dE} = \frac{\langle \sigma_A v \rangle}{2} J_{\Delta\Omega} \frac{R_{sc} \rho_{sc}^2}{4\pi m_\chi^2} \frac{dN}{dE},$$

where $\langle \sigma_A v \rangle$ is the velocity-averaged DM self-annihilation cross-section, R_{sc} is the radius of solar circle ($R_{sc} = 8.5\text{kpc}$) and ρ_{sc} is local DM density ($\rho_{sc} = \rho(R_{sc})$). The factor 1/2 accounts for DM being its own antiparticle, $1/4\pi$ is for isotropic emission of the annihilation products, m_χ is assumed mass of the DM particle and dN/dE is the spectrum of

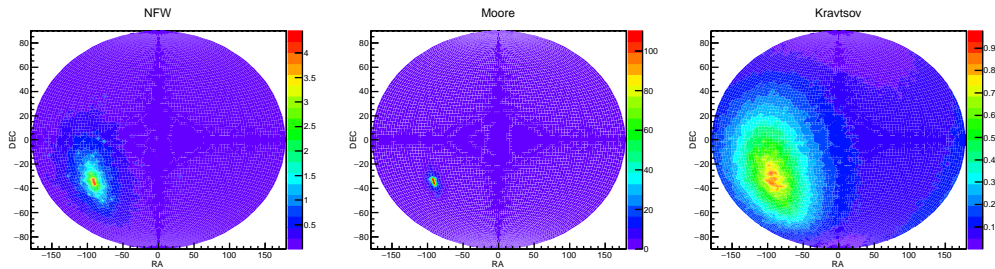


Fig. 3. – Spherical projections of the expected signal shape for DM annihilation scenario in equatorial coordinate system (Right Ascension, Declination) for NFW, Moore and Kravtsov profiles. The normalization was chosen arbitrarily.

the annihilation products. For decaying DM the intensity of the products is proportional to density and expected neutrino flux is then:

$$(2) \quad \frac{d\Phi_{\Delta\Omega}}{dE} = \frac{1}{\tau} J_{d\Delta\Omega} \frac{R_{sc}\rho_{sc}}{4\pi m_\chi} \frac{dN}{dE},$$

where τ is the DM particle lifetime.

In the presented analysis four annihilation/decay channels are considered: $\nu\bar{\nu}$, $b\bar{b}$, W^+W^- , $\mu^+\mu^-$. As a model independent approach 100% branching ratio to a given annihilation/decay mode is assumed. In annihilation into pairs of $\nu\bar{\nu}$, spectrum of neutrinos per flavour is a monochromatic line with $dN/dE = \frac{2}{3}\delta(E - m_\chi)$, where the prefactor 2/3 arises under the assumption that 2 neutrinos are produced per one annihilation of DM particles pair and all neutrino flavours are equally populated. Differential multiplicity spectra for other considered DM annihilation modes ($b\bar{b}$, W^+W^- , $\mu^+\mu^-$) were obtained using the DarkSUSY simulator [9]. For calculation of the DM induced neutrino flux at the detector a full mixing is assumed due to long-baseline oscillations over the galactic scales. The expected number of neutrino events observed in the detector can be found by integrating the differential neutrino flux $\frac{d\Phi_{\Delta\Omega}}{dE}$ over the detector livetime and the direction- and energy-dependent effective area.

Since the calculation of the angular and energy spectra of DM annihilation/decay products is well established [8], one can try to simulate neutrino events originating in these processes. In order to simulate these events, reweighting procedure was applied to generated atmospheric Monte Carlo (MC). Neutrino interactions at SK are simulated with large statistics corresponding to 500 years of livetime for each running period of SK-I, SK-II, SK-III and SK-IV. After reweighting the expected DM induced neutrino intensity, angular distribution and energy spectra are reproduced. The results of the simulation, presented in Fig. 3, are consistent with expectations. For each halo model, the signal is peaked and pointing towards the GC direction. The angular resolution of the detector is taken into account. The difference between profiles can be clearly seen in case of DM annihilation scenario. Therefore, one expects differences in obtained results due to differences in adopted halo model.

4. – Analysis idea

Dark matter induced neutrino flux would manifest itself through a large scale anisotropy with the largest excess of neutrino flux at the area of the GC, as it is shown in previous section. To test this hypothesis, two regions on the sky are chosen. The on-source region is centered on the GC position (266° Right Ascension, -29° Declination) and defined by a circle around this point with a half-opening angle Ψ . The off-source region is equally-sized, but offset by 180° in Right Ascension (see Fig. 4). In both regions signal and

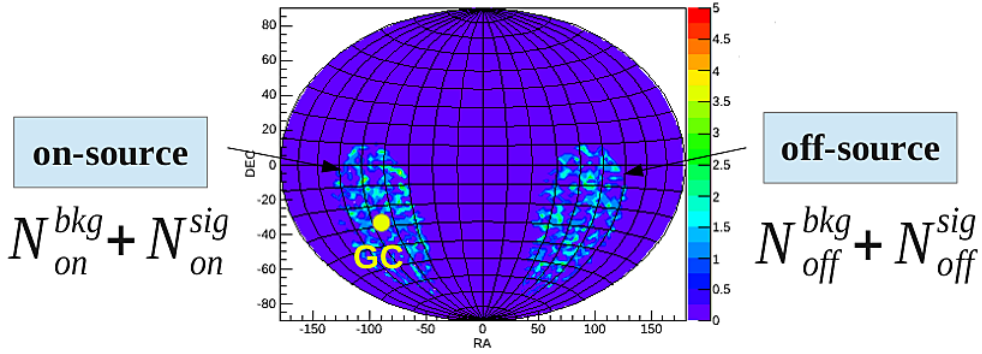


Fig. 4. – Schematic explanation of the analysis idea. The difference in total number of events between two regions of the sky will be considered.

background events are expected. Signal events are defined as the DM induced neutrinos. Background events consist of atmospheric neutrinos which are expected to be equally distributed in the on- and off-source regions. Therefore, the difference in number of neutrino events between on- and off-source regions should contain no background events. In this way the background can be estimated directly from the data. This method is independent on atmospheric MC simulations and related systematic uncertainties as they should equally affect on- and off-source regions. The difference in number of neutrino events between on- and off-source regions corresponds to the difference in signal events:

$$(3) \quad \Delta N = (N_{on}^{bkg} + N_{on}^{sig}) - (N_{off}^{bkg} + N_{off}^{sig}) \approx N_{on}^{sig} - N_{off}^{sig} = \Delta N^{sig},$$

and is directly proportional to the DM self-annihilation cross-section $\langle \sigma_A v \rangle$ and inversely proportional to lifetime τ in decaying DM scenario.

The angular resolution of the detector strongly depends on the energy of parent neutrinos. Leptons produced in interactions of low energy neutrinos (≤ 1 GeV) loosely follow the direction of the parent neutrino. Therefore, it would be good to find optimal size of the on-source region so that signal to background ratio is maximal. The optimization was performed for NFW profile, which was a benchmark model in this analysis. The angular resolution of the detector differs between event classes and the optimization was carried out separately for SubGeV and MultiGeV FC, PC and UPMU event samples based entirely on simulated events. The rest of the analysis was based only on data.

5. – Results

5.1. Upper limits on dark matter induced neutrinos. – The comparison between number of observed neutrino events ($\nu_\mu\bar{\nu}_\mu$) in on- and off-source regions is shown in Table I for DM annihilation case and in Table II for DM decay. Different event classes (FC, PC and UPMU) were considered separately, and for each class, the optimal size of on-source region was determined based on the simulated DM induced neutrino events (see previous section). No excess of events has been observed. This is the main result of the performed analysis, which can be further interpreted under the assumptions of various DM halo models. Based on the null results in the considered samples (corresponding to various M_χ), one can derive the upper limit on the number of DM induced neutrinos. In the last column of Tab. I and II, the 90% C.L. limit on the allowed difference in number of signal events between two considered regions is calculated using the Bayesian approach (see [10] for detailed description).

TABLE I. – *The number of neutrino events ($\nu_\mu\bar{\nu}_\mu$) observed in on-source and corresponding off-source regions for each considered event classes. The optimal size of the on-source region was determined separately for each class. The last column shows the upper 90% Confidence Level (C.L) limit on the allowed difference in number of signal events between two considered regions. Results for DM annihilation scenario.*

Sample	Size [°]	On-source	Off-source	ΔN_{sig}	90% CL ΔN_{sig}
μ -like FC SubGeV	80	3604	3656	-49 ± 85.2	113.5
μ -like FC MultiGeV	30	226	243	-17 ± 21.7	26.8
PC	20	75	77	-2 ± 12.3	19.0
UPMU	10	50.2*	64.0*	-13.8 ± 10.7	11.1
ALL	35	1988.4	2125.5	-137.1 ± 64.1	51.6

TABLE II. – *The same as in Table I, but for DM decay scenario.*

Sample	Size [°]	On-source	Off-source	ΔN_{sig}	90% CL ΔN_{sig}
μ -like FC SubGeV	80	3604	3656	-49 ± 85.2	113.5
μ -like FC MultiGeV	80	1479	1417	62 ± 53.8	134.9
PC	80	1043	985	58 ± 45.0	118.3
UPMU	80	3144.0*	3204.2*	-60.2 ± 79.7	99.6
ALL	80	9270.0	9259.2	10.8 ± 136.1	230.6

* In case of UPMU samples, estimated rate of bkg events due to horizontal cosmic ray muons is subtracted from the final data set.

5.2. Upper limits on dark matter induced ($\nu_\mu\bar{\nu}_\mu$) neutrino flux. – At this point one can try to interpret obtained results in terms of limits on DM induced neutrino flux, taking into account given annihilation channel and halo model. It is possible to translate upper limit on a difference in number of DM induced neutrinos $\Delta N_{90\%}^{sig}$ to corresponding difference in average DM induced neutrino fluxes between on-source ($\frac{d\Phi_{\Delta\Omega_{on}}}{dE}$) and off-

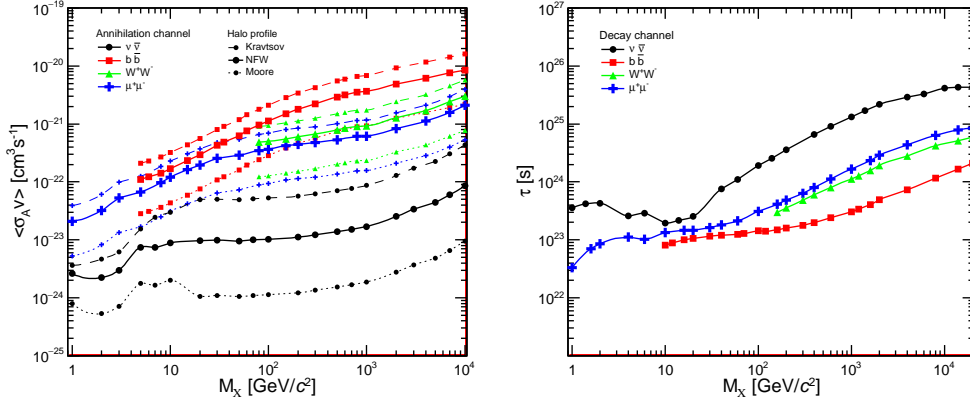


Fig. 5. – Left plot: The upper 90% C.L. limits on DM self-annihilation cross section for considered annihilation channels, for NFW, Moore and Kravtsov profiles. Regions above the lines are excluded. Each time 100% BR to a given annihilation channel is assumed. Right plot: The same but for the lower limits on DM particles lifetime.

source ($\frac{d\Phi_{\Delta\Omega_{off}}}{dE}$) regions:

$$(4) \quad \Delta N_{90\%}^{sig} \rightarrow \frac{d\Phi_{\Delta\Omega_{on}}}{dE} - \frac{d\Phi_{\Delta\Omega_{off}}}{dE}.$$

Using atmospheric MC, one can match the number of observed atmospheric events N_{atm} with corresponding true value of neutrino flux $\frac{d\Phi_{atm}}{dE}$ for a given neutrino energy and the same relation can be obtained for signal events.

5.3. Upper limits on dark matter self-annihilation cross section and lower limits on dark matter particles lifetime. – Based on theoretical expectations about DM halo model, one can translate the limit on the DM induced neutrino flux $\frac{d\Phi_{\Delta\Omega}}{dE}$ into the upper limit for velocity-averaged self-annihilation cross-section $\langle\sigma_{A}v\rangle$ (Eq. 1). The upper limits can be evaluated for NFW, Moore and Kravtsov profiles, using different average signal intensities $J_{\Delta\Omega}$. The results for three considered profiles are presented in Fig. 5 (left plot). The derived constraints on the value of $\langle\sigma_{A}v\rangle$ strongly depend on adopted halo model. Obtained differences between benchmark model (NFW) and models used as extreme cases (Moore and Kravtsov) can reach the order of magnitude.

In analogical way one can calculate limits on DM particles lifetime (Eq. 2). In this case, there is no point to consider different DM halo models, because the expected signal intensity $J_{d\Delta\Omega}$ is on the same level. Results are presented in Fig. 5 (right plot).

6. – Summary

Dark matter search is a highly challenging field, encompassing very different experimental techniques and detection methods. The existing results from other experiments, which are not conclusive, demonstrate the importance of a multi-messenger approach to dark matter searches and validate the interest in a neutrino channel.

Self-annihilating or decaying DM in our Galaxy might produce neutrinos. This would manifest in a large-scale anisotropy of observed neutrino flux. The excess of DM induced neutrinos over the atmospheric neutrino background is expected from the direction of the GC due to increased DM density in this region. It is convenient to search for this effect in equatorial coordinate system as the position of the GC is fixed in these coordinates. The direction and energy spectrum of neutrinos produced in DM annihilation/decay remains unchanged during their propagation throughout the Galaxy. Therefore, neutrinos can be a powerful tool in DM searches.

In the presented analysis we search for global anisotropy in neutrino flux which has not been found. Based on a null contribution of DM induced neutrinos, the upper limits for DM velocity-averaged self-annihilation cross section $\langle\sigma_{Av}\rangle$ and lower limits for lifetime τ for various masses of relic particles in range 1GeV - 10 TeV were derived.

REFERENCES

- [1] ASHIE Y. *et al.* (THE SUPER-KAMIOKANDE COLLABORATION), *Phys. Rev. Lett. D*, **71** (2005) 112005;
- [2] FUKUDA S. *et al.* (THE SUPER-KAMIOKANDE COLLABORATION), *Nucl. Instruments and Methods A*, **501** (2003) 418;
- [3] NAVARRO J., FRENK C. and WHITE S., *Astrophysical Journal*, **462** (1996) 563;
- [4] MOORE B. *et al.*, *Mon. Not. Roy. Astron. Soc.*, **310** (1999) 1147;
- [5] KRAVTSOV A. *et al.*, *Astrophysical Journal*, **502** (1998) 48;
- [6] DIEMAND J., KUHLEN M. and MADAU P, *Astrophys. Journal*, **667** (2007) 859;
- [7] MASSEY R. *et al.*, *Nature*, **445** (2007) 286-290;
- [8] YUKSEL H. *et al.*, *Phys. Rev. D*, **76** (2007) 123506;
- [9] GONDOLO P., EDSJ J., ULLIO P., BERGSTRM L., SCHELKE M. and BALTZ E.A, *JCAP*, **07** (2004) 008;
- [10] BARNETT R. *et al.* (THE PARTICLE DATA GROUP), *Phys. Rev.D*, **54** (1996) 164;